Title

Hepatic Src Homology Phosphatase 2 Regulates Energy Balance in Mice

Journal

Endocrinology, 153(7)

ISSN

0888-8809

Authors

Nagata, Naoto
Matsuo, Kosuke
Bettaieb, Ahmed
et al.

Publication Date

2012-07-01

DOI

10.1210/en.2012-1406

Peer reviewed

Hepatic Src Homology Phosphatase 2 Regulates Energy Balance in Mice

Naoto Nagata,* Kosuke Matsuo,* Ahmed Bettaieb, Jesse Bakke, Izumi Matsuo, James Graham, Yannan Xi, Siming Liu, Alexey Tomilov, Natalia Tomilova, Susan Gray, Dae Young Jung, Jon J. Ramsey, Jason K. Kim, Gino Cortopassi, Peter J. Havel, and Fawaz G. Haj

Department of Nutrition (N.N., K.M., A.B., J.B., I.M., J.G., Y.X., S.L., P.J.H., F.G.H.), University of California Davis, Davis, California 95616; Department of Molecular Biosciences (J.G., A.T., N.T., J.J.R., G.C., P.J.H.), School of Veterinary Medicine, University of California Davis, Davis, California 95618; and Program in Molecular Medicine (S.G., D.Y.J., J.K.K.) and Department of Medicine (J.K.K.), Division of Endocrinology, Metabolism and Diabetes, University of Massachusetts Medical School, Worcester, Massachusetts 01605

The Src homology 2 domain-containing protein-tyrosine phosphatase Src homology phosphatase 2 (Shp2) is a negative regulator of hepatic insulin action in mice fed regular chow. To investigate the role of hepatic Shp2 in lipid metabolism and energy balance, we determined the metabolic effects of its deletion in mice challenged with a high-fat diet (HFD). We analyzed body mass, lipid metabolism, insulin sensitivity, and glucose tolerance in liver-specific Shp2-deficient mice (referred to herein as LSHKO) and control mice fed HFD. Hepatic Shp2 protein expression is regulated by nutritional status, increasing in mice fed HFD and decreasing during fasting. LSHKO mice gained less weight and exhibited increased energy expenditure compared with control mice. In addition, hepatic Shp2 deficiency led to decreased liver steatosis, enhanced insulin-induced suppression of hepatic glucose production, and impeded the development of insulin resistance after high-fat feeding. At the molecular level, LSHKO exhibited decreased hepatic endoplasmic reticulum stress and inflammation compared with control mice. In addition, tyrosine and serine phosphorylation of total and mitochondrial signal transducer and activator of transcription 3 were enhanced in LSHKO compared with control mice. In line with this observation and the increased energy expenditure of LSHKO, oxygen consumption rate was higher in liver mitochondria of LSHKO compared with controls. Collectively, these studies identify hepatic Shp2 as a novel regulator of systemic energy balance under conditions of high-fat feeding. (***Endocrinology*** **153: 3158–3169, 2012)**

Obesity is a major health problem worldwide, and obese individuals exhibit a higher risk of chronic diseases, such as cardiovascular disease, nonalcoholic fatty liver disease (NAFLD), and type 2 diabetes mellitus (1–3). Currently, there are few therapies for targeting obesity and its associated comorbidities in humans. Thus, elucidating the mechanisms underlying obesity is vital for understanding its pathogenesis and developing effective therapies. Genetic and molecular studies identified tyrosine phosphorylation as a key regulator of energy balance and glucose homeostasis (4–6).

Tyrosine phosphorylation is tightly controlled by the opposing actions of protein-tyrosine kinases and protein-tyrosine phosphatases (PTP) (7). Src homology phospha-

ISSN Print 0013-7227 ISSN Online 1945-7170
Printed in U.S.A.

doi: 10.1210/en.2012-1406 Received April 11, 2012. Accepted April 30, 2012.
First Published Online May 22, 2012

* N.N. and K.M. contributed equally to the work.

Abbreviations: AUC, Area under the curve; BAT, brown adipose tissue; ER, endoplasmic reticulum; GTT, glucose tolerance test; H&E, hematoxylin-eosin; HET, heterozygous; HFD, high-fat diet; HGP, hepatic glucose production; ITT, insulin tolerance test; JNK, c-Jun N-terminal kinase; LSHKO, liver-specific Shp2 knockout; NAFLD, nonalcoholic fatty liver disease; PKC, protein kinase C; PGC1α, peroxisome proliferator-activated receptor γ coactivator-1α; PTP, protein-tyrosine phosphatase; SH, Src homology; Shp2, Src homology phosphatase 2; SREBP, sterol regulatory element binding protein; STAT3, signal transducer and activator of transcription 3.

tase 2 (Shp2) is a broadly expressed nontransmembrane PTP that plays an essential role in most receptor tyrosine kinase signaling pathways (8–10). *In vivo* studies provided insights into the physiological role of Shp2 in insulin signaling and glucose homeostasis. Targeted mutation of Shp2 exon 3 in mice leads to embryonic lethality (11), precluding studies of the effects of global Shp2 deletion. Hemizygous mice are viable but do not manifest any apparent defects in insulin action (12). Transgenic mice that express a dominant negative mutant of Shp2 in skeletal muscle, liver, and adipose tissue exhibit insulin resistance and impaired insulin-stimulated glucose uptake (13). In addition, Shp2 deletion in striated and cardiac muscle results in insulin resistance, impaired glucose uptake in muscle cells, and glucose intolerance (14, 15). Moreover, Shp2 deletion in the pancreas causes defective glucose-stimulated insulin secretion and impaired glucose tolerance (16). On the other hand, mice lacking Shp2 in the liver exhibit increased hepatic insulin action and enhanced systemic insulin sensitivity (17). The improved insulin sensitivity is caused, at least in large part, by attenuation of direct dephosphorylation of insulin receptor substrate 1/2 in the liver and concomitant increase in phosphatidylinositol 3 kinase/Akt signaling (17).

Shp2 has been implicated in energy balance and body mass regulation (18, 19). *In vitro* studies reveal that Shp2 promotes signaling from Tyr985 of the leptin receptor, leading to enhanced activation of the Erk pathway (20, 21). These findings are supported by studies in mice with selective deletion of Shp2 in postmitotic forebrain neurons that develop leptin resistance and early onset obesity (22). In addition, another line of neuronal Shp2 deletion also exhibits obesity and insulin resistance (23). Moreover, mice with proopiomelanocortin neuron-specific Shp2 deletion exhibit decreased leptin sensitivity and elevated adiposity, implicating Shp2 as an important component of proopiomelanocortin neuron regulation of energy balance (24). Together, these studies highlight the function of neuronal Shp2 in energy balance. However, the role of Shp2 in peripheral tissues in systemic energy balance, if any, remains to be determined.

In this study, we investigated the metabolic effects of hepatic Shp2 deficiency in mice challenged with high-fat feeding. We determined alterations in body mass, energy balance, glucose homeostasis and lipid metabolism and delineated the underlying molecular mechanisms.

Materials and Methods

Mouse studies

Shp2 floxed ($Shp2^{fl/fl}$) mice were generated previously (25). Albumin-Cre mice were obtained from C. R. Kahn (Joslin Diabetes Center/Harvard University, Boston, MA). All mice studied were age-matched males on a mixed 129Sv/J x C57Bl/6J background and were maintained on a 12-h light, 12-h dark cycle with free access to water and food. Mice were fed standard lab chow (no. 5001; Purina, St. Louis, MO) at weaning and switched to high-fat diet (HFD) (60% kcal from fat, no. D12492; Research Diets, New Brunswick, NJ) at 6 wk of age. Genotyping for the Shp2 floxed allele and for the presence of Cre was performed by PCR, using DNA extracted from tails (17). Mice were euthanized by cervical dislocation, and the liver, spleen, kidney, heart, pancreas, epididymal, retroperitoneal, mesenteric, subcutaneous, and brown adipose depots were collected and weighed. A portion of each liver was snap frozen in liquid nitrogen for biochemical studies while another portion was fixed in buffered formalin for hematoxylin-eosin (H&E) staining. All mouse studies were approved by the Institutional Animal Care and Use Committee at University of California Davis.

Metabolic measurements

Biochemical parameters, energy expenditure, mitochondrial oxygen consumption rates, assessment of insulin sensitivity and glucose tolerance, and hyperinsulinemic-euglycemic clamps were performed as detailed in Supplementary Methods, published on The Endocrine Society's Journals Online web site at http://endo.endojournals.org.

Biochemical analyses

For biochemical studies, 32-wk-old male mice fed HFD for 26 wk were fasted overnight and then killed. Tissues were ground in liquid nitrogen and lysed using radioimmunoprecipitation assay buffer as we previously described (17). Proteins were resolved by SDS-PAGE and transferred to polyvinylidene fluoride membranes. Immunoblot of lysates was performed with primary antibodies (Supplemental Table 1), and after incubation with appropriate secondary antibodies, proteins were visualized using chemiluminescence (Bio-Rad, Hercules, CA). Pixel intensities of immunoreactive bands were quantified using FluorChem 9900 (Alpha Innotech, Santa Clara, CA). Expression of lipogenic genes was assessed by quantitative real-time PCR (iCycler; Bio-Rad) using SYBR Green with appropriate primers (Supplemental Table 2) as we described previously (17).

Statistical analyses

Data are expressed as mean ± SEM. Statistical analyses were performed using JMP8 software (SAS Institute, Cary, NC). Comparisons between groups were made by unpaired two-tailed Student's *t* test. A symbol (*) indicates $P \leq 0.05$, whereas a duplicate symbol (**) indicates $P \leq 0.01$. Insulin tolerance tests (ITT) and glucose tolerance tests (GTT) were analyzed by repeated measures ANOVA. *Post hoc* analysis was performed using Tukey-Kramer honestly significant difference test.

Results

Nutritional regulation of hepatic Shp2 expression

Hepatic Shp2 deficiency alters glucose homeostasis in mice fed regular chow (17). To further investigate the metabolic functions of hepatic Shp2, we challenged mice with

prolonged (26 wk) high-fat feeding. Subsequently, we determined alterations in hepatic inflammation, endoplasmic reticulum (ER) stress, and Shp2 expression. Consistent with published studies (26, 27), immunoblots of liver lysates revealed increased hepatic TNFα expression in wild-type mice fed HFD compared with those fed regular chow, suggesting elevated inflammatory response (Fig. 1A). In addition, binding immunoglobulin protein expression was increased in mice fed HFD compared with those fed regular chow, suggesting increased ER stress response. Notably, Shp2 expression was elevated (~2-fold) in livers of mice fed HFD compared with those fed regular chow. Similarly, expression of another PTP known to regulate hepatic insulin signaling, PTP1B (28), was increased in mice fed HFD (Fig. 1A). Next, we investigated the effects of fasting and refeeding on hepatic Shp2 expression. Shp2 protein expression decreased in the livers of fasted mice but returned to control (fed) levels upon refeeding (Fig. 1B). In line with published reports (29, 30), fasting led to increased hepatic peroxisome proliferator-activated receptor γ coactivator-1α (PGC1α) and decreased PTP1B expression. Together, these findings demonstrate that hepatic Shp2 expression is regulated by nutritional status in mice.

Given the nutritional regulation of hepatic Shp2 expression, we generated mice with liver-specific Shp2 deletion as we previously described (17) and challenged them with HFD. Briefly, albumin-Cre Shp2$^{fl/+}$ mice were crossed to Shp2$^{fl/fl}$ mice, yielding Alb-Cre Shp2$^{fl/fl}$ [liver-specific Shp2 knockout (LSHKO)], Alb-Cre Shp2$^{fl/+}$ [heterozygous (HET)], and Shp2$^{fl/fl}$ (control; fl/fl) mice. Immunoblot analysis of liver lysates from mice fed HFD indicated that Shp2 protein expression was decreased by approximately 55% in HET and approximately 85% in

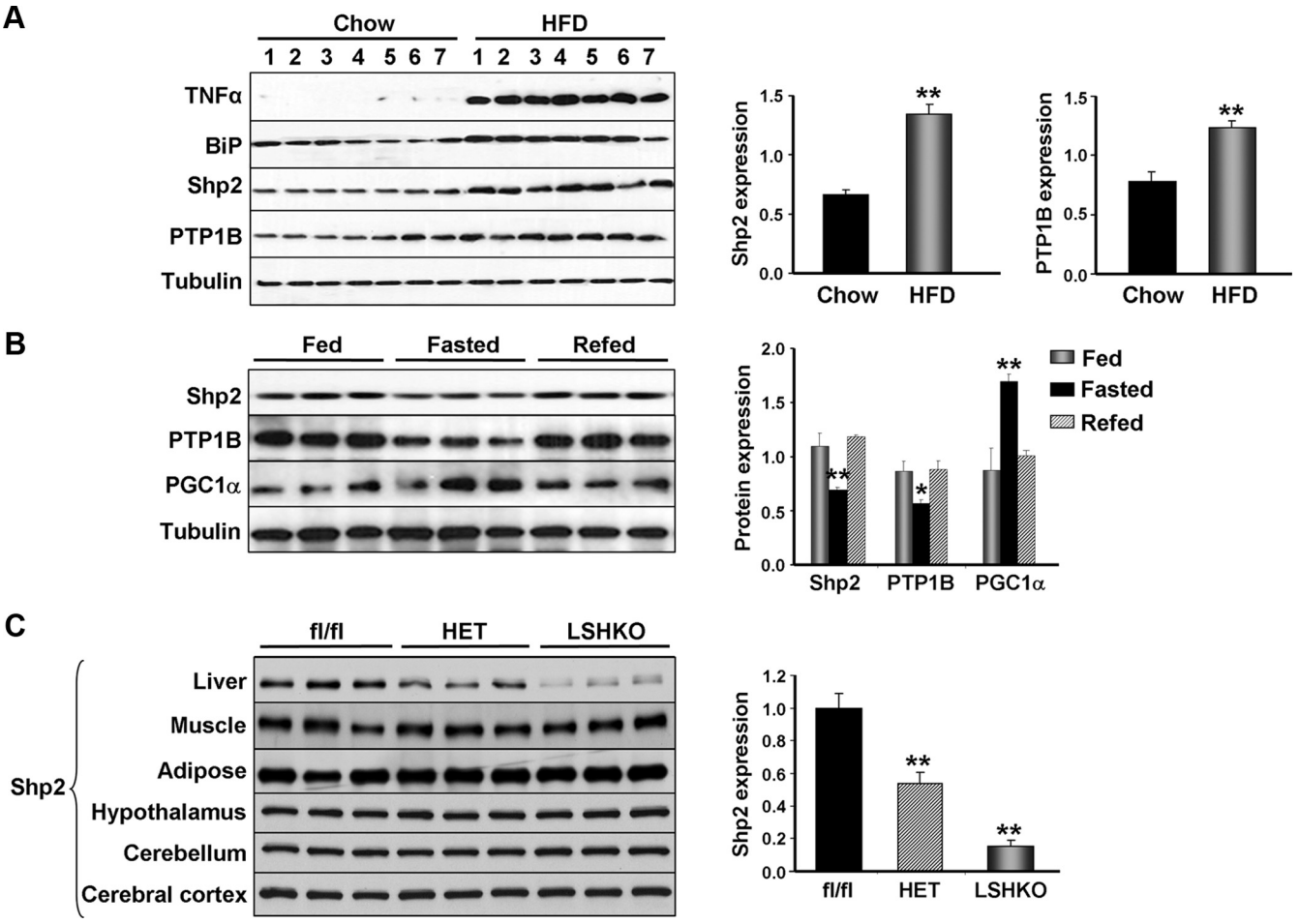

FIG. 1. Nutritional regulation of hepatic Shp2 protein expression. A, Immunoblot of TNFα, binding immunoglobulin protein (BiP), Shp2, and PTP1B expression in liver lysates of wild-type male mice (32 wk old) fed regular chow and HFD (for 26 wk). Lysates were also probed for tubulin as a loading control. *Each lane* represents liver lysates from a different animal. *Bar charts* represent Shp2 and PTP1B protein expression normalized to tubulin. B, Immunoblot of Shp2, PTP1B, and PGC1α in liver lysates of male mice (34 wk old) that were fed regular chow *ad libitum* (fed), fasted for 24 h (fasted), or fasted for 24 h followed by 14 h of feeding (refed). *Bar charts* represent Shp2, PTP1B, and PGC1α protein expression normalized to tubulin. C, Immunoblot of Shp2 expression in various tissues from Shp2$^{fl/fl}$ (fl/fl), Alb-Cre Shp2$^{fl/+}$ (HET), and Alb-Cre Shp2$^{fl/fl}$ (LSHKO) mice. *Bar chart* represents hepatic Shp2 expression normalized to tubulin. Data were analyzed by two-tailed Student's *t* test, and results represent mean ± SEM. *, Significant difference between chow and HFD (A), fasted and fed (B), and HET and LSHKO *vs.* fl/fl (C).

LSHKO compared with control (Fig. 1C). This is consistent with complete deletion of Shp2 in hepatocytes, and the residual expression is likely due to the presence of other cell types in the liver as we previously indicated (17). Shp2 expression was unchanged in muscle, adipose tissue, and brain (hypothalamus, cerebellum, and cerebral cortex), indicating specificity of deletion. Thus, LSHKO mice provide a useful tool to dissect the effects of hepatic Shp2 deficiency on HFD-induced metabolic damage.

Decreased body weight and adiposity in LSHKO mice fed HFD

To investigate whether hepatic Shp2 deficiency affects systemic energy balance, we determined body weights of mice fed HFD. Body weights of LSHKO were significantly lower than those of control mice, and by the end of the study, LSHKO mice weighed 12% less than controls (Fig. 2A). Similar findings were observed in three other independent cohorts of mice (data not shown). In addition, food intake was comparable between LSHKO and control mice fed HFD (Supplemental Fig. 1A). Moreover, bomb calorimetry revealed a trend for decreased energy in feces of LSHKO compared with control mice, suggesting possible increase in intestinal absorption in LSHKO mice (Supplemental Fig. 1B). To determine the tissue(s) that contributes to decreased body weight in LSHKO mice, we performed body composition analysis. Liver, mesenteric, and subcutaneous fat depots and kidney weights (adjusted to body weight) were significantly lower in LSHKO compared with control mice (Fig. 2B). In line with decreased fat mass, LSHKO exhibited lower leptin concentrations compared with control mice (Table 1). Although Shp2 has been implicated in growth hormone signaling (31), comparable head-rump length and hepatic IGF-I mRNA were observed in LSHKO and control mice, suggesting no alterations in growth hormone signaling (Supplemental Fig. 1, C and D).

To investigate the mechanism underlying decreased body weight of LSHKO mice, we determined energy expenditure of 27-wk-old LSHKO and control mice in open-circuit indirect calorimetry cages as described in Supple-

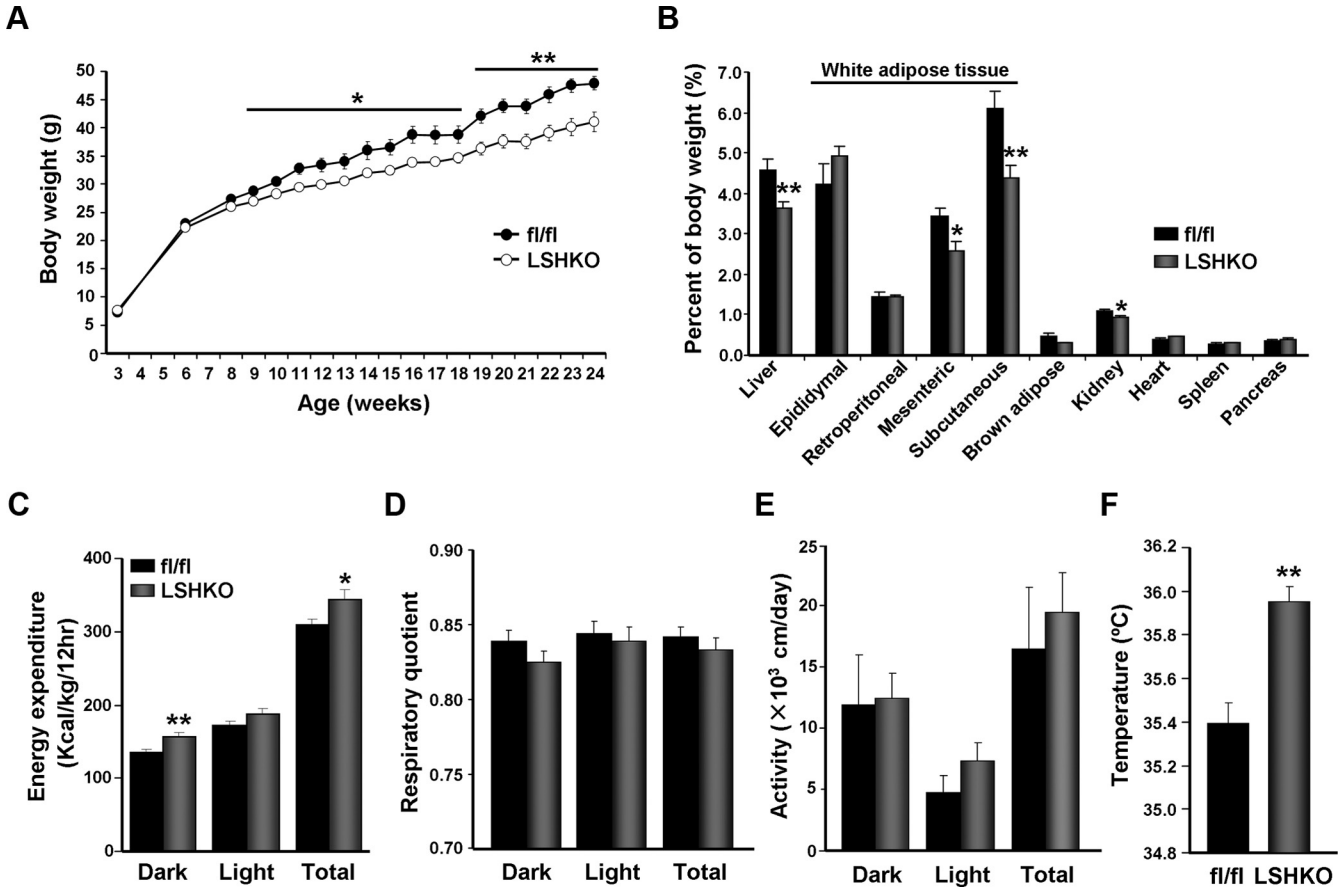

FIG. 2. Decreased body weight and increased energy expenditure in LSHKO mice fed HFD. A, Body weights of fl/fl (n = 8) and LSHKO (n = 9) mice fed HFD from 6 wk of age. B, Tissue weight is presented as percentage of body weight. Energy expenditure (C), respiratory quotient (D), and total activity (E) in fl/fl (n = 8) and LSHKO (n = 8) mice during dark and light cycles. *Bar graphs* of energy expenditure and respiratory quotient represent AUC calculations. F, Average rectal temperature in fl/fl (n = 7) and LSHKO (n = 7) mice at 23 wk of age measured in three consecutive days. Data were analyzed by two-tailed Student's *t* test, and results represent the mean ± SEM. *, Significant difference between fl/fl and LSHKO.

TABLE 1. Metabolic parameters of fl/fl and LSHKO mice fed HFD for 8 wk

Metabolic parameters	fl/fl (n = 8)	LSHKO (n = 8)
Blood glucose (mg/dl)		
Fed	179.4 ± 6.2	143.1 ± 7.6[b]
Fasted	116.3 ± 14.6	88.4 ± 4.3
Serum insulin (ng/ml)		
Fed	3.38 ± 1.30	1.65 ± 0.31
Fasted	0.34 ± 0.11	0.17 ± 0.03
Leptin (ng/ml) fed	93.2 ± 14.1	46.0 ± 5.7[a]
Free fatty acids (mM) fed	0.38 ± 0.03	0.31 ± 0.01[a]

Statistical analysis was performed using unpaired, two-tailed Student's *t* test.

[a] Difference between fl/fl and LSHKO mice; *, $P \leq 0.05$.

[b] Difference between fl/fl and LSHKO mice; **, $P \leq 0.01$.

mental Methods. Energy expenditure was significantly elevated in LSHKO compared with control mice, particularly during the dark cycle, when mice are more active and the thermic effect of food is highest (Fig. 2C). In addition, LSHKO exhibited a trend for decreased respiratory quotient (Fig. 2D), and increased locomotor activity (Fig. 2E) compared with control mice, but these did not reach statistical significance. Consistent with their increased energy expenditure, LSHKO displayed a significant increase in body temperature compared with control mice (Fig. 2F). Together, these findings indicate that the decreased body weight of LSHKO mice fed HFD is due, at least in part, to increased energy expenditure.

Hepatic Shp2 deficiency reduces steatosis, ER stress, and inflammation in mice fed HFD

HFD causes accumulation of lipids in the liver, a process that leads to fatty liver disease (also known as NAFLD) and eventually to nonalcoholic steatohepatitis (32). H&E staining of liver sections of control mice fed HFD for 26 wk revealed micro- and macrosteatosis (Fig. 3A). In contrast, LSHKO mice presented with a lower number of

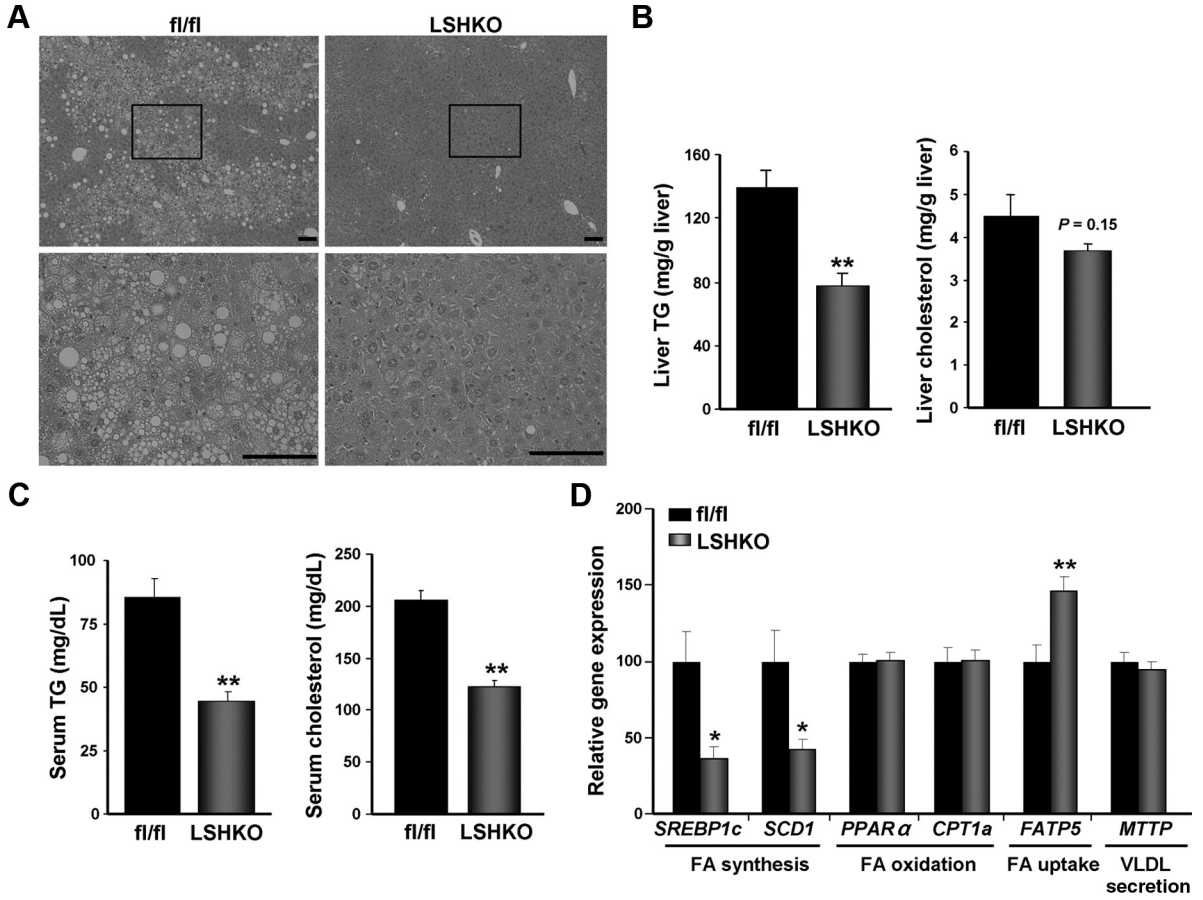

FIG. 3. Decreased liver steatosis and dyslipidemia in LSHKO mice fed HFD. A, Liver sections from fl/fl and LSHKO mice fed HFD at 32 wk of age were analyzed by H&E staining. *Boxed regions* in the *upper panel* are magnified in *lower panel*. *Scale bars*, 100 μm. B, Hepatic triglyceride and cholesterol of fl/fl (n = 8) and LSHKO (n = 8) mice. C, Serum triglyceride and cholesterol were measured at 14 wk of age. D, Quantitative real-time PCR determination of mRNA of genes implicated in fatty acids (FA) synthesis, oxidation, uptake, and very low-density lipoprotein (VLDL) secretion (normalized against 36B4) in livers of fl/fl (n = 8) and LSHKO (n = 8) mice. Total RNA was extracted from the same liver samples used for lipids measurement. Results represent the mean ± SEM and were analyzed by two-tailed Student's *t* test. *, Significant difference between fl/fl and LSHKO. PPARα, peroxisome proliferator-activated receptor α; CPT1a, carnitine palmitoyltransferase 1a; MTTP, microsomal triglyceride transfer protein; FATP5, fatty acid transporter member 5; TG, triglyceride.

lipid droplets and with small diameter. Consistent with this observation, liver triglyceride content was significantly lower in LSHKO compared with control mice (Fig. 3B) and comparable with LSHKO mice fed regular chow (77.7 ± 8.4 mg/g liver) as we previously reported (17). In addition, liver cholesterol content tended to be lower in LSHKO compared with control mice but did not reach statistical significance (Fig. 1B). Serum triglyceride, cholesterol, and free fatty acid concentrations were significantly lower in LSHKO compared with control mice (Fig. 3C and Table 1). Consistent with histological findings, hepatic mRNA of lipogenic genes, such as sterol regulatory element binding protein (SREBP)-1c and stearoyl-Coenzyme A desaturase 1, was significantly lower in LSHKO compared with control mice (Fig. 3D). However, mRNA of genes for β-oxidation, such as peroxisome proliferator-activated receptor α and carnitine palmitoyltransferase 1a, and genes for very low-density lipoprotein secretion, such as microsomal triglyceride transfer protein, was comparable in the livers of LSHKO and control mice. On the other hand, hepatic mRNA of fatty acid transporter member 5, exclusively expressed in the liver, was significantly increased in LSHKO compared with control mice possibly due to compensation for decreased *de novo* fatty acids synthesis. We further investigated whether hepatic Shp2 deficiency mitigates HFD-induced ER stress and inflammation. Cells use adaptive mechanisms to mitigate ER stress known as the unfolded protein response (33). Unfolded protein response is triggered by proteins on the ER: protein kinase RNA-dependent-like ER-regulated kinase, inositol-requiring protein 1α, and activating transcription factor 6 (34). If the adaptive mechanisms fail to preserve homeostasis, then this will lead to inflammation and hepatosteatosis (35, 36). In addition, a major mediator of metabolic dysfunction in adiposity is cellular inflammation, and up-regulation of inflammation is detrimental to proper insulin signaling (37). Immunoblot analyses of liver lysates revealed significant reduction in hepatic ER stress and inflammation markers in LSHKO compared with control mice (Supplemental Fig. 2). Together, these findings indicate that hepatic Shp2 deficiency mitigates HFD-induced steatohepatitis and might confer protection against the development of hyperlipidemia.

LSHKO mice are protected against HFD-induced insulin resistance

Mice with acute or chronic hepatic Shp2 deletion fed regular chow exhibit increased insulin sensitivity compared with controls without alterations in body weight (17). To further examine the effects of hepatic Shp2 deficiency on glucose homeostasis, we tested whether its deletion mitigates HFD-induced insulin resistance. We assayed several metabolic parameters in LSHKO and control mice (Table 1). LSHKO exhibited significantly lower fed blood glucose, and a trend toward decreased fasting glucose compared with control mice suggesting increased insulin sensitivity. Consistent with this observation, LSHKO mice exhibited a trend toward decreased fed and fasted serum insulin concentrations, although these did not reach statistical significance. These data suggest that LSHKO have increased systemic insulin sensitivity compared with control mice. To directly assess insulin sensitivity, mice were subjected to ITT at different stages of high-fat feeding. LSHKO exhibited significantly greater reduction in blood glucose after insulin injection compared with control mice [area under the curve (AUC), fl/fl 10,059 ± 632 *vs.* LSHKO 7112 ± 345% X min; $P < 0.01$] (Fig. 4A). In addition, LSHKO mice showed increased ability to clear glucose from the peripheral circulation during GTT (AUC, fl/fl 35,987 ± 2174 *vs.* LSHKO 28,558 ± 1599 mg/dl·min; $P = 0.02$) (Fig. 4B). Comparable differences were preserved in older (20 wk old) mice (AUC in ITT: fl/fl 7775 ± 461 *vs.* LSHKO 6110 ± 544% X min, $P = 0.04$; AUC in GTT: fl/fl 39,353 ± 2343 *vs.* LSHKO 31,583 ± 1865 mg/dl·min, $P = 0.02$) (Supplemental Fig. 3, A and B). There was no significant difference in insulin secretion between LSHKO and control mice during GTT (data not shown). In line with increased insulin sensitivity, LSHKO exhibited enhanced insulin-induced hepatic Akt Ser473 phosphorylation compared with control mice (Supplemental Fig. 3C).

To gain further insight into the underlying mechanism of enhanced insulin sensitivity, we performed hyperinsulinemic-euglycemic clamps in LSHKO mice fed HFD for 14 wk. Basal hepatic glucose production (HGP) was not different in control and LSHKO mice. However, insulin failed to suppress HGP during the clamp in control mice, consistent with the severe hepatic insulin resistance evoked by chronic high-fat feeding (Fig. 4C). In contrast, HGP was almost completely suppressed in LSHKO mice during clamps (insulin-stimulated state), resulting in higher insulin-mediated suppression of HGP in LSHKO mice (Fig. 4, C and D). Moreover, the glucose infusion rate required to maintain euglycemia during clamps was higher in LSHKO mice, suggesting an improvement in whole-body insulin response (Fig. 4E). Insulin-stimulated whole-body glucose turnover was similar in the two groups, indicating no difference in glucose uptake between control and LSHKO mice (Fig. 4F). Whole-body glycogen and lipid synthesis and whole-body glycolysis also were comparable between the two groups (Supplemental Fig. 3, D and E). As expected from our study, blood glucose tended to be lower in LSHKO mice under basal conditions, but

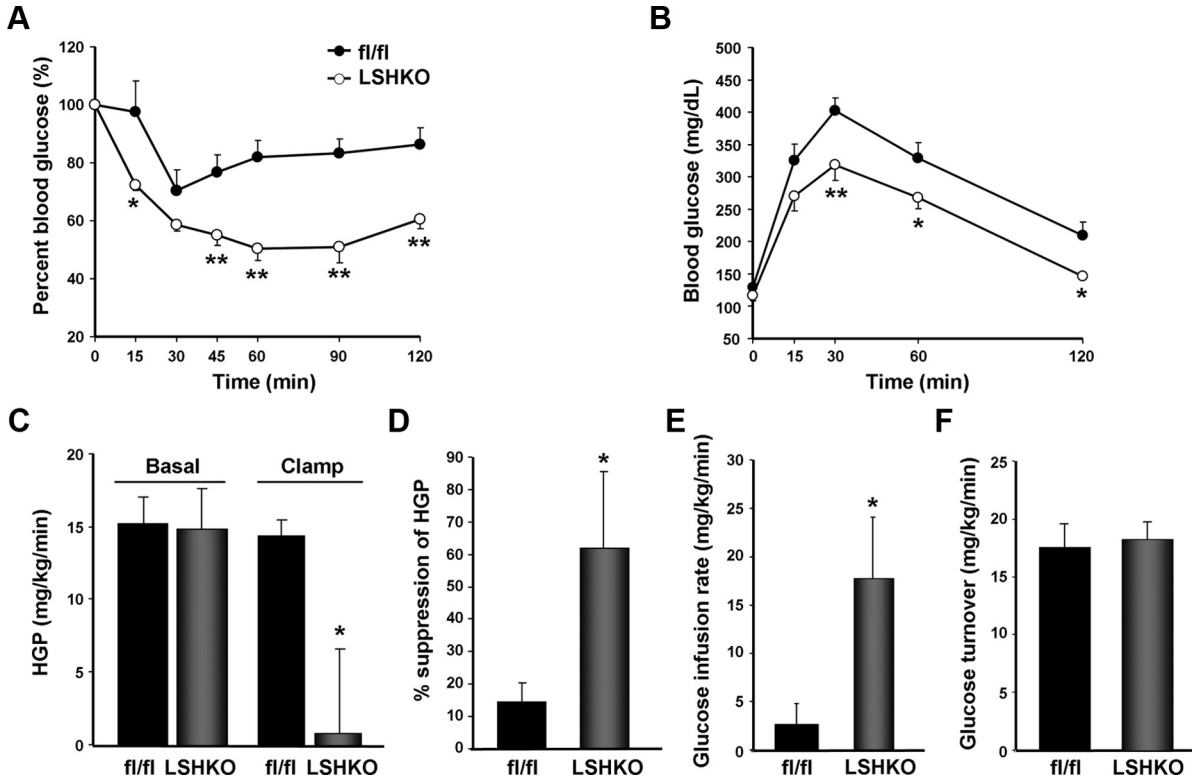

FIG. 4. Improved insulin sensitivity and glucose tolerance in LSHKO mice fed HFD. A, ITT (0.7 mU/g body weight) on fl/fl (n = 8) and LSHKO (n = 7) mice fed HFD at 9 wk of age. Data are expressed as percentage change of initial value. B, GTT (1.2 mg/g body weight) on fl/fl (n = 8) and LSHKO (n = 8) mice at 12 wk of age. Results represent the mean ± SEM, and data were analyzed by repeated measures ANOVA and Tukey-Kramer honestly significant difference test. C–F, Hyperinsulinemic-euglycemic clamps were performed on fl/fl (n = 5) and LSHKO (n = 5) mice fed HFD. C, HGP under basal and clamp conditions. D, Insulin-mediated percent suppression of HGP. E, Glucose infusion rate during clamps. F, Insulin-stimulated whole-body glucose turnover. Statistical analysis was performed using one-tailed Student's *t* test. *, Significant difference between fl/fl and LSHKO mice.

this difference did not reach statistical significance (Supplemental Fig. 3F). However, circulating insulin was significantly lower in LSHKO mice at baseline (Supplemental Fig. 3G). Taken together, these findings reveal that hepatic Shp2 deficiency attenuates the development of HFD-induced insulin resistance.

Increased hepatic signal transducer and activator of transcription 3 (STAT3) phosphorylation in HFD-fed LSHKO mice

To delineate the molecular basis for increased energy expenditure in LSHKO mice, we assessed STAT3 phosphorylation. Shp2 was implicated in regulating STAT3 (Tyr705) phosphorylation in mouse heart (15) and liver (38). Of note, STAT3 is activated by phosphorylation at Tyr705, leading to its dimerization and relocation to the nucleus to promote gene expression (39). In addition, phosphorylation at Ser727 is required for maximal transcriptional activity of STAT3 (40, 41). Importantly, STAT3 Ser727 phosphorylation is required for its mitochondrial actions and regulation of oxidative phosphorylation (41, 42). Immunoblot of liver lysates from fasted mice revealed that STAT3 (Tyr705) phosphorylation, normalized to STAT3 expression, was increased in LSHKO compared with control mice (Fig. 5A), consistent with published data (15, 38). Moreover, STAT3 (Ser727) phosphorylation was increased in liver lysates of LSHKO compared with control mice. We further investigated STAT3 phosphorylation in mitochondrial fractions of the liver (Fig. 5B). Mitochondrial STAT3 (Ser727) phosphorylation was significantly increased in LSHKO compared with control mice, and Shp2 was detected in liver mitochondria as previously reported (43).

STAT3 (Ser727) can be phosphorylated by several kinases, such as Erk, c-Jun N-terminal kinase (JNK), mammalian target of rapamycin/p70S6K, and protein kinase Cδ (PKCδ) (40, 44). Thus, we examined whether these serine kinases were implicated in the elevated STAT3 (Ser727) phosphorylation in LSHKO mice. Immunoblot analysis revealed that p-ERK (Thr202/Tyr204) and p-JNK (Thr183/Tyr185) were significantly decreased in LSHKO compared with control mice (Fig. 5C). In addition, phosphorylation of p70S6K (Thr389) and its substrate S6 ribosomal protein (Ser235/236) were comparable between LSHKO and control mice at fasted conditions. In contrast,

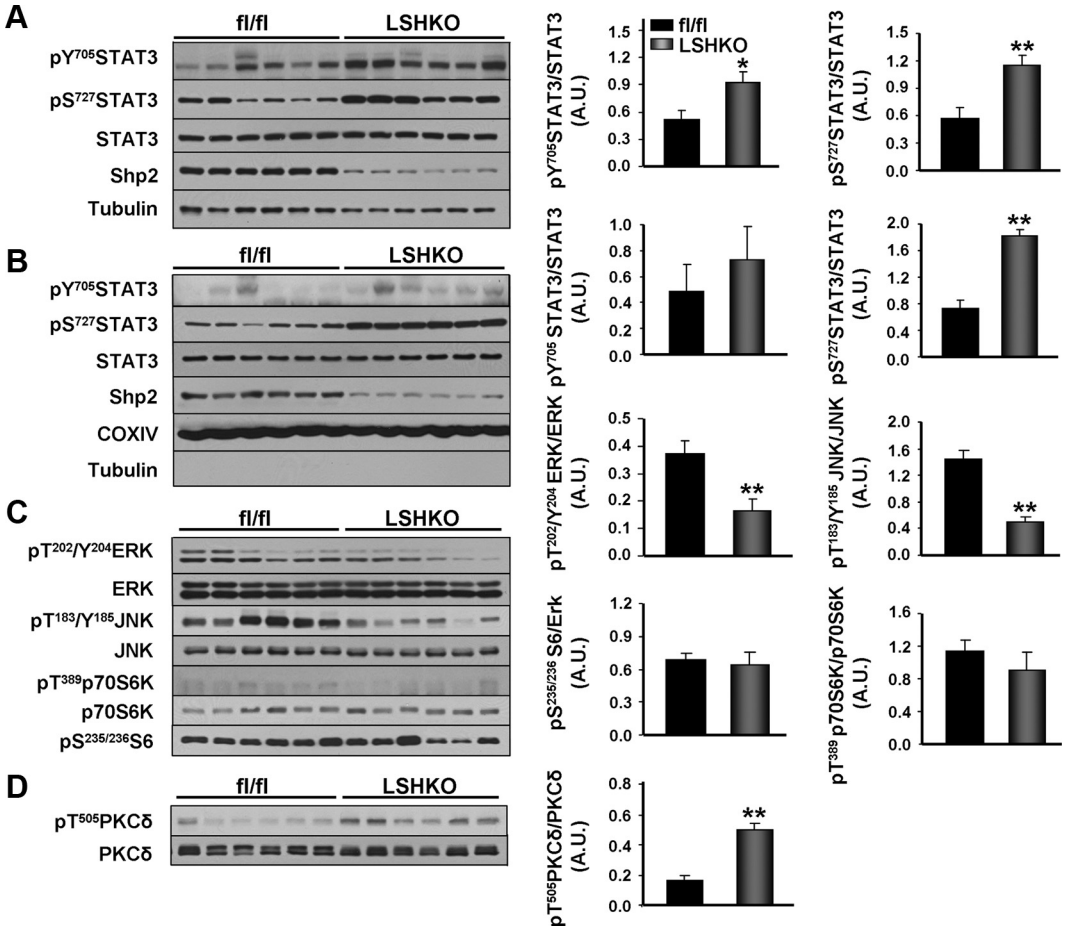

FIG. 5. Increased hepatic STAT3 phosphorylation in LSHKO mice fed HFD. Immunoblots of p-STAT3 (Tyr705 and Ser727), STAT3, Shp2, and tubulin in liver lysates of fasted mice (A) and isolated liver mitochondria (B). Mitochondrial proteins were also probed for cytochrome c oxidase subunit IV (COXIV) and tubulin to check the purity of the samples. Immunoblot analysis of p-ERK (Thr202/Tyr204), ERK, p-JNK (Thr183/Tyr185), JNK, p-p70S6K (Thr389), p70S6K, and p-S6 (Ser235/236) (C) and p-PKCδ (Thr505) and PKCδ (D) using liver lysates. *Each lane* represents liver lysates from a different fasted animal. *Bar graphs* represent normalized data for p-STAT3/STAT3, p-ERK/ERK, p-JNK/JNK, p-S6/Erk, p-p70S6K/p70S6K, and p-PKCδ/PKCδ from two independent experiments and presented as mean ± SEM. Statistical analysis was performed using two-tailed Student's *t* test. *, Significant difference between fl/fl and LSHKO mice. A.U., Arbitrary unit.

phosphorylation of PKCδ (Thr505), which is important for catalytic activity (45), was significantly increased in LSHKO compared with control mice (Fig. 5D). Together, these findings demonstrate elevated phosphorylation of total and mitochondrial STAT3 in LSHKO mice and suggest that this might contribute to increased energy expenditure.

Increased mitochondrial respiration in HFD-fed LSHKO mice

STAT3 (Ser727) phosphorylation is required for STAT3 mitochondrial actions and regulation of oxidative phosphorylation (41, 42). To test whether increased STAT3 (Ser727) phosphorylation in LSHKO mice contributes to mitochondrial respiratory function, we measured oxygen consumption rate in liver mitochondria of LSHKO and control mice using the Seahorse XF24 analyzer. When pyruvate/malate was used to determine complex I-driven respiration, ADP-stimulated (state III) respiration rates were significantly increased (~20%) in LSHKO compared with control mice (Fig. 6A). The maximal respiratory capacity was comparable, and reserve respiratory capacity tended to be lower in LSHKO compared with control mice but did not reach statistical significance (Fig. 6A). On the other hand, succinate-induced state III respiration, which represents complex II-driven respiration, maximal respiratory capacity, and reserve capacity, was not changed by hepatic Shp2 deficiency (Fig. 6B). In addition, LSHKO exhibited a significantly increased capacity for complex III-linked reactive oxygen species production compared with control mice, because reactive oxygen spices production was not increased in these mice when complex I was fully reduced (pyr/mal + rotenone) but was observed when both complex I and III were reduced (pyr/mal + antimycin A and

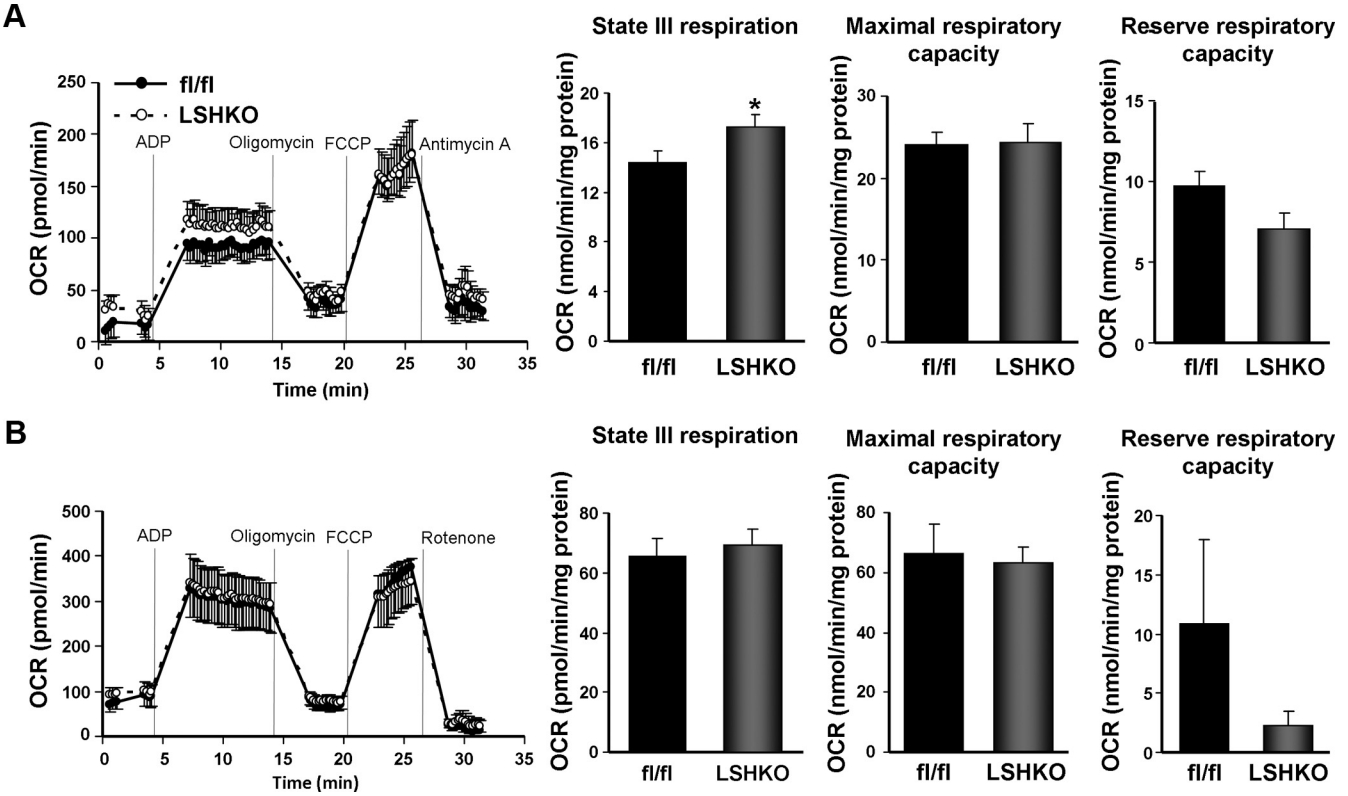

FIG. 6. Increased oxygen consumption rate in isolated mitochondria from liver of LSHKO mice fed HFD. A, Bioenergetic profile of isolated liver mitochondria from LSHKO and fl/fl (n = 6 per group) mice fed HFD at 32 wk of age using pyruvate as the substrate in presence of malate. State III respiration was induced by ADP, proton leak-driven respiration was accessed by oligomycin, and respiratory capacity was measured as carbonyl cyanide-p-trifluoromethoxyphenylhydrazone (FCCP)-induced respiration. *Bar graphs* represent oxygen consumption rate (OCR) for indicated rates of oxygen consumption; 7.5 μg of protein were used per well. B, Bioenergetic profile of mitochondria was assayed by using succinate as the substrate in the presence of rotenone; 5 μg of protein were used per well. Each mouse liver was assayed in pentaplicate. Statistical analysis was performed using two-tailed Student's *t* test (*, $P \leq 0.05$).

succinate + antimycin A) (Supplemental Fig. 4). Additional studies are required to further delineate the regulation of mitochondrial function by Shp2. Together, these data demonstrate that hepatic Shp2 modulates mitochondrial function, including respiration and electron transport in the liver of mice fed HFD, and this may contribute, at least in part, to the increased energy expenditure in LSHKO mice.

Discussion

Obesity is a leading cause of several debilitating diseases, such as type 2 diabetes mellitus and NAFLD (1–3). To develop effective therapies for these diseases, it is important to elucidate the underlying molecular mechanisms. In this study, we report that hepatic Shp2 deficiency mitigated HFD-induced metabolic damage. LSHKO mice fed HFD gained less weight than controls and exhibited decreased liver steatosis. In addition, hepatic Shp2 deficiency impeded the development of HFD-induced insulin resistance. At the molecular level, LSHKO mice exhibited decreased hepatic ER stress and inflammation, and increased STAT3 phosphorylation compared with controls. Collectively, these findings demonstrate a novel role for hepatic Shp2 in metabolic homeostasis and systemic energy balance.

Hepatic Shp2 expression is dynamically regulated by nutritional status in mice, increasing with high-fat feeding and decreasing during fasting. The underlying reason(s) for this regulation remain to be determined but is likely to involve several factors, such as insulin sensitivity and/or inflammation, among others. Previous studies demonstrate that Shp2 expression and activity are increased in livers of diabetic rats (46). However, factors other than insulin resistance can also regulate PTP expression *in vivo*. Indeed, inflammation is a contributing factor underlying PTP1B overexpression in diabetes and obesity *in vivo* (47). Given the role of Shp2 in regulating TNF receptor and IL-6 signaling (48), HFD-induced inflammatory responses might contribute to hepatic Shp2 overexpression. Importantly, the increased expression of Shp2 after high-fat feeding raises the possibility that hepatic Shp2 inhibition/

deficiency might protect against HFD-induced metabolic damage, as demonstrated by the current study. Additional studies are required to fully elucidate the mechanism(s) underlying nutritional regulation of hepatic Shp2 expression.

Mice with hepatic Shp2 deficiency gained less weight on HFD compared with controls. This was due, in large part, to increased energy expenditure in LSHKO mice. At the molecular level, the increased hepatic STAT3 phosphorylation in LSHKO mice could contribute to their systemic energy expenditure. Hepatic STAT3 deletion leads to insulin resistance and increased adiposity and body weight (49). In addition, STAT3 (Ser727) phosphorylation is required for STAT3 mitochondrial actions, where it promotes the activity of electron transport chain that generates energy by oxidative phosphorylation (41, 42). The current data suggest that STAT3 (Ser727) phosphorylation in LSHKO mice could be regulated by PKCδ, but additional studies are required to elucidate the mechanisms of STAT3 regulation in LSHKO mice. At any rate, the observed biochemical alterations translate to regulation of respiratory function. Increased respiration using pyruvate as a substrate suggests that LSHKO mice liver mitochondria have increased proton flux through complex I, which is important for utilization of $NADH+H^+$ produced by the tricarboxylic acid cycle and by β-oxidation in mitochondria (Supplemental Fig. 5). It is important to note that we cannot rule out that the increased insulin sensitivity in LSHKO mice contributes to their decreased body mass. Indeed, both PKCδ (Thr505) phosphorylation and activation (50) and pyruvate dehydrogenase activity are regulated by insulin signaling (Supplemental Fig. 5). Finally, the contribution of extrahepatic tissues to the increased energy expenditure in LSHKO mice remains to be determined. Brown adipose tissue (BAT) and skeletal muscle oxidize fatty acids through β-oxidation and produce heat by uncoupling and ATP by oxidative phosphorylation (51, 52). Expression of uncoupling proteins and genes involved in β-oxidation, such as carnitine palmitoyltransferase 1b and medium chain acyl-coenzyme A dehydrogenase in BAT and skeletal muscle was comparable in LSHKO and control mice (Supplemental Fig. 6). This suggests that increased energy expenditure in LSHKO mice is unlikely due to increased uncoupling proteins expression and β-oxidation in BAT and/or skeletal muscle.

LSHKO mice fed HFD exhibited reduced hepatic steatosis compared with controls. The current study provides insights into potential underlying mechanisms that include, but are not limited to, hepatic STAT3, ER stress signaling, and inflammation. STAT3 activation suppresses SREBP-1c promoter activity and decreases SREBP-1c protein expression in hepatocytes (53–55), suggesting that STAT3 activation can attenuate lipogenesis and subsequent inflammation caused by steatosis. In line with these reports, we demonstrated elevated hepatic STAT3 phosphorylation and decreased mRNA of lipogenic genes in LSHKO compared with control mice. ER stress has been observed in livers of murine models of obesity (26) and patients with nonalcoholic steatohepatitis (56). Importantly, chemical chaperones that enhance the ER functional capacity reduce hepatic steatosis, indicating that they are useful for the treatment of NAFLD (57). The current *in vivo* studies demonstrate for the first time that hepatic Shp2 deficiency affects both eukaryotic translation initiation factor 2α and inositol-requiring protein 1α subarms of ER stress. Finally, in obesity, inflammatory cytokines promote steatosis through the inhibition of insulin signaling and SREBP-1c activation (58, 59). Our studies demonstrated that LSHKO mice exhibited decreased hepatic expression of inflammation cytokines compared with controls. Although we cannot exclude the possibility that decreased hepatic ER stress and inflammation in LSHKO mice are secondary to decreased body mass, our data suggest that alterations in these pathways might account, at least in part, for the protective effects of hepatic Shp2 deficiency against steatosis and HFD-induced metabolic damage.

LSHKO mice exhibited enhanced ability of insulin to suppress HGP, improved systemic insulin sensitivity and glucose tolerance compared with control mice fed HFD. The lower body mass of LSHKO mice raises the possibility that their improved insulin sensitivity is secondary to body mass. However, a number of observations argue against this notion. 1) If there was global improvement in insulin sensitivity in response to lower body weight in LSHKO mice on HFD, one would expect secondary increase in muscle insulin sensitivity in these mice. However, our clamp studies indicate that there is no increase in whole-body glucose turnover in LSHKO mice on HFD. Furthermore, LSHKO exhibited similar basal and insulin-induced Akt activation (as determined by Ser473 phosphorylation) in skeletal muscle compared with control mice (data not shown), suggesting no significant improvement in muscle insulin action. 2) Previously, we reported that LSHKO mice fed regular chow exhibited improved insulin sensitivity, whereas body weight and body fat were comparable with controls (17). 3) And similarly, improved insulin sensitivity was observed in mice with adenovirus-mediated deletion of hepatic Shp2 fed regular chow, where body weights were comparable with controls (17). Taken together, these findings suggest that the protection against HFD-induced insulin resistance in LSHKO mice is likely a primary effect and not secondary to reduced body weight.

In summary, the current study demonstrates that hepatic Shp2 is implicated in the regulation of lipid and glu-

cose metabolism and systemic energy balance. These findings suggest that selective hepatic Shp2 inhibition might have beneficial effects in the treatment of type 2 diabetes and management of disorders associated with the metabolic syndrome, including dysplipidemia and NAFLD.

Acknowledgments

We thank Dr. C. Ronald Kahn (Joslin Diabetes Center, Boston, MA) for Alb-Cre mice, Dr. Marc Montminy (Salk Institute, San Diego, CA) for PGC1α antibodies, and Dr. Benjamin Neel (Ontario Cancer Institute, Toronto, Ontario, Canada) for Shp2$^{fl/fl}$ mice and advice.

Address all correspondence and requests for reprints to: Fawaz G. Haj, D.Phil., University of California Davis, 3135 Meyer Hall, Davis, California 95616. E-mail: fghaj@ucdavis.edu.

This work was supported by grants from the Center for Health and Nutrition Research (University of California Davis), the American Diabetes Association Junior Faculty Award 7-06-JF-28), the Juvenile Diabetes Research Foundation Research Grant 1-2009-337, and National Institutes of Health (NIH) Grants R56DK084317 and RO1DK090492 (to F.G.H.) and RO1 DK080742 (to S.G.), and the UMass Mouse Phenotyping Center Grant NIDDK DK32520 (to J.K.K.). P.J.H.'s laboratory receives funding from NIH Grants HL075675, HL09133, and DK087307.

Disclosure Summary: The authors have nothing to disclose.

References

1. **Friedman JM** 2000 Obesity in the new millennium. Nature 404: 632–634
2. **Spiegelman BM, Flier JS** 2001 Obesity and the regulation of energy balance. Cell 104:531–543
3. **Ahima RS** 2006 Obesity epidemic in need of answers. Gastroenterology 131:991
4. **Nandi A, Kitamura Y, Kahn CR, Accili D** 2004 Mouse models of insulin resistance. Physiol Rev 84:623–647
5. **Taniguchi CM, Emanuelli B, Kahn CR** 2006 Critical nodes in signalling pathways: insights into insulin action. Nat Rev Mol Cell Biol 7:85–96
6. **Friedman JM, Halaas JL** 1998 Leptin and the regulation of body weight in mammals. Nature 395:763–770
7. **Tonks NK** 2006 Protein tyrosine phosphatases: from genes, to function, to disease. Nat Rev Mol Cell Biol 7:833–846
8. **Sugimoto S, Lechleider RJ, Shoelson SE, Neel BG, Walsh CT** 1993 Expression, purification, and characterization of SH2-containing protein tyrosine phosphatase, SH-PTP2. J Biol Chem 268:22771–22776
9. **Feng GS** 2007 Shp2-mediated molecular signaling in control of embryonic stem cell self-renewal and differentiation. Cell Res 17: 37–41
10. **Chan G, Kalaitzidis D, Neel BG** 2008 The tyrosine phosphatase Shp2 (PTPN11) in cancer. Cancer Metastasis Rev 27:179–192
11. **Saxton TM, Henkemeyer M, Gasca S, Shen R, Rossi DJ, Shalaby F, Feng GS, Pawson T** 1997 Abnormal mesoderm patterning in mouse embryos mutant for the SH2 tyrosine phosphatase Shp-2. EMBO J 16:2352–2364
12. **Arrandale JM, Gore-Willse A, Rocks S, Ren JM, Zhu J, Davis A, Livingston JN, Rabin DU** 1996 Insulin signaling in mice expressing reduced levels of Syp. J Biol Chem 271:21353–21358
13. **Maegawa H, Hasegawa M, Sugai S, Obata T, Ugi S, Morino K, Egawa K, Fujita T, Sakamoto T, Nishio Y, Kojima H, Haneda M, Yasuda H, Kikkawa R, Kashiwagi A** 1999 Expression of a dominant negative SHP-2 in transgenic mice induces insulin resistance. J Biol Chem 274:30236–30243
14. **Kontaridis MI, Yang W, Bence KK, Cullen D, Wang B, Bodyak N, Ke Q, Hinek A, Kang PM, Liao R, Neel BG** 2008 Deletion of Ptpn11 (Shp2) in cardiomyocytes causes dilated cardiomyopathy via effects on the extracellular signal-regulated kinase/mitogen-activated protein kinase and RhoA signaling pathways. Circulation 117:1423–1435
15. **Princen F, Bard E, Sheikh F, Zhang SS, Wang J, Zago WM, Wu D, Trelles RD, Bailly-Maitre B, Kahn CR, Chen Y, Reed JC, Tong GG, Mercola M, Chen J, Feng GS** 2009 Deletion of Shp2 tyrosine phosphatase in muscle leads to dilated cardiomyopathy, insulin resistance, and premature death. Mol Cell Biol 29:378–388
16. **Zhang SS, Hao E, Yu J, Liu W, Wang J, Levine F, Feng GS** 2009 Coordinated regulation by Shp2 tyrosine phosphatase of signaling events controlling insulin biosynthesis in pancreatic β-cells. Proc Natl Acad Sci USA 106:7531–7536
17. **Matsuo K, Delibegovic M, Matsuo I, Nagata N, Liu S, Bettaieb A, Xi Y, Araki K, Yang W, Kahn BB, Neel BG, Haj FG** 2010 Altered glucose homeostasis in mice with liver-specific deletion of Src homology phosphatase 2. J Biol Chem 285:39750–39758
18. **Neel BG, Gu H, Pao L** 2003 The 'Shp'ing news: SH2 domain-containing tyrosine phosphatases in cell signaling. Trends Biochem Sci 28:284–293
19. **Feng GS** 2006 Shp2 as a therapeutic target for leptin resistance and obesity. Expert Opin Ther Targets 10:135–142
20. **Carpenter LR, Farruggella TJ, Symes A, Karow ML, Yancopoulos GD, Stahl N** 1998 Enhancing leptin response by preventing SH2-containing phosphatase 2 interaction with Ob receptor. Proc Natl Acad Sci USA 95:6061–6066
21. **Bjørbaek C, Buchholz RM, Davis SM, Bates SH, Pierroz DD, Gu H, Neel BG, Myers Jr MG, Flier JS** 2001 Divergent roles of SHP-2 in ERK activation by leptin receptors. J Biol Chem 276:4747–4755
22. **Zhang EE, Chapeau E, Hagihara K, Feng GS** 2004 Neuronal Shp2 tyrosine phosphatase controls energy balance and metabolism. Proc Natl Acad Sci USA 101:16064–16069
23. **Krajewska M, Banares S, Zhang EE, Huang X, Scadeng M, Jhala US, Feng GS, Krajewski S** 2008 Development of diabesity in mice with neuronal deletion of Shp2 tyrosine phosphatase. Am J Pathol 172: 1312–1324
24. **Banno R, Zimmer D, De Jonghe BC, Atienza M, Rak K, Yang W, Bence KK** 2010 PTP1B and SHP2 in POMC neurons reciprocally regulate energy balance in mice. J Clin Invest 120:720–734
25. **Zhang SQ, Yang W, Kontaridis MI, Bivona TG, Wen G, Araki T, Luo J, Thompson JA, Schraven BL, Philips MR, Neel BG** 2004 Shp2 regulates SRC family kinase activity and Ras/Erk activation by controlling Csk recruitment. Mol Cell 13:341–355
26. **Ozcan U, Cao Q, Yilmaz E, Lee AH, Iwakoshi NN, Ozdelen E, Tuncman G, Görgün C, Glimcher LH, Hotamisligil GS** 2004 Endoplasmic reticulum stress links obesity, insulin action, and type 2 diabetes. Science 306:457–461
27. **Matveyenko AV, Gurlo T, Daval M, Butler AE, Butler PC** 2009 Successful versus failed adaptation to high-fat diet-induced insulin resistance: the role of IAPP-induced β-cell endoplasmic reticulum stress. Diabetes 58:906–916
28. **Delibegovic M, Zimmer D, Kauffman C, Rak K, Hong EG, Cho YR, Kim JK, Kahn BB, Neel BG, Bence KK** 2009 Liver-specific deletion of protein-tyrosine phosphatase 1B (PTP1B) improves metabolic

syndrome and attenuates diet-induced endoplasmic reticulum stress. Diabetes 58:590–599
29. **Yoon JC, Puigserver P, Chen G, Donovan J, Wu Z, Rhee J, Adelmant G, Stafford J, Kahn CR, Granner DK, Newgard CB, Spiegelman BM** 2001 Control of hepatic gluconeogenesis through the transcriptional coactivator PGC-1. Nature 413:131–138
30. **Sun C, Zhang F, Ge X, Yan T, Chen X, Shi X, Zhai Q** 2007 SIRT1 improves insulin sensitivity under insulin-resistant conditions by repressing PTP1B. Cell Metab 6:307–319
31. **Maile LA, Clemmons DR** 2002 Regulation of insulin-like growth factor I receptor dephosphorylation by SHPS-1 and the tyrosine phosphatase SHP-2. J Biol Chem 277:8955–8960
32. **Perlemuter G, Bigorgne A, Cassard-Doulcier AM, Naveau S** 2007 Nonalcoholic fatty liver disease: from pathogenesis to patient care. Nat Clin Pract Endocrinol Metab 3:458–469
33. **Kaufman RJ, Scheuner D, Schröder M, Shen X, Lee K, Liu CY, Arnold SM** 2002 The unfolded protein response in nutrient sensing and differentiation. Nat Rev Mol Cell Biol 3:411–421
34. **Ron D, Walter P** 2007 Signal integration in the endoplasmic reticulum unfolded protein response. Nat Rev Mol Cell Biol 8:519–529
35. **Ji C, Kaplowitz N** 2006 ER stress: can the liver cope? J Hepatol 45:321–333
36. **Kaplowitz N, Than TA, Shinohara M, Ji C** 2007 Endoplasmic reticulum stress and liver injury. Semin Liver Dis 27:367–377
37. **Hotamisligil GS** 2010 Endoplasmic reticulum stress and the inflammatory basis of metabolic disease. Cell 140:900–917
38. **Bard-Chapeau EA, Yuan J, Droin N, Long S, Zhang EE, Nguyen TV, Feng GS** 2006 Concerted functions of Gab1 and Shp2 in liver regeneration and hepatoprotection. Mol Cell Biol 26:4664–4674
39. **Schindler C, Levy DE, Decker T** 2007 JAK-STAT signaling: from interferons to cytokines. J Biol Chem 282:20059–20063
40. **Decker T, Kovarik P** 2000 Serine phosphorylation of STATs. Oncogene 19:2628–2637
41. **Wegrzyn J, Potla R, Chwae YJ, Sepuri NB, Zhang Q, Koeck T, Derecka M, Szczepanek K, Szelag M, Gornicka A, Moh A, Moghaddas S, Chen Q, Bobbili S, Cichy J, Dulak J, Baker DP, Wolfman A, Stuehr D, Hassan MO, Fu XY, Avadhani N, Drake JI, Fawcett P, Lesnefsky EJ, Larner AC** 2009 Function of mitochondrial Stat3 in cellular respiration. Science 323:793–797
42. **Myers Jr MG** 2009 Cell biology. Moonlighting in mitochondria. Science 323:723–724
43. **Salvi M, Stringaro A, Brunati AM, Agostinelli E, Arancia G, Clari G, Toninello A** 2004 Tyrosine phosphatase activity in mitochondria: presence of Shp-2 phosphatase in mitochondria. Cell Mol Life Sci 61:2393–2404
44. **Novotny-Diermayr V, Zhang T, Gu L, Cao X** 2002 Protein kinase Cδ associates with the interleukin-6 receptor subunit glycoprotein (gp) 130 via Stat3 and enhances Stat3-gp130 interaction. J Biol Chem 277:49134–49142
45. **Steinberg SF** 2004 Distinctive activation mechanisms and functions for protein kinase Cδ. Biochem J 384:449–459
46. **Ahmad F, Goldstein BJ** 1995 Alterations in specific protein-tyrosine phosphatases accompany insulin resistance of streptozotocin diabetes. Am J Physiol 268:E932–E940
47. **Zabolotny JM, Kim YB, Welsh LA, Kershaw EE, Neel BG, Kahn BB** 2008 Protein-tyrosine phosphatase 1B expression is induced by inflammation in vivo. J Biol Chem 283:14230–14241
48. **You M, Flick LM, Yu D, Feng GS** 2001 Modulation of the nuclear factor κB pathway by Shp-2 tyrosine phosphatase in mediating the induction of interleukin (IL)-6 by IL-1 or tumor necrosis factor. J Exp Med 193:101–110
49. **Inoue H, Ogawa W, Ozaki M, Haga S, Matsumoto M, Furukawa K, Hashimoto N, Kido Y, Mori T, Sakaue H, Teshigawara K, Jin S, Iguchi H, Hiramatsu R, LeRoith D, Takeda K, Akira S, Kasuga M** 2004 Role of STAT-3 in regulation of hepatic gluconeogenic genes and carbohydrate metabolism in vivo. Nat Med 10:168–174
50. **Le Good JA, Ziegler WH, Parekh DB, Alessi DR, Cohen P, Parker PJ** 1998 Protein kinase C isotypes controlled by phosphoinositide 3-kinase through the protein kinase PDK1. Science 281:2042–2045
51. **Cannon B, Nedergaard J** 2004 Brown adipose tissue: function and physiological significance. Physiol Rev 84:277–359
52. **Rasmussen BB, Wolfe RR** 1999 Regulation of fatty acid oxidation in skeletal muscle. Annu Rev Nutr 19:463–484
53. **Ueki K, Kondo T, Tseng YH, Kahn CR** 2004 Central role of suppressors of cytokine signaling proteins in hepatic steatosis, insulin resistance, and the metabolic syndrome in the mouse. Proc Natl Acad Sci USA 101:10422–10427
54. **Kroy DC, Beraza N, Tschaharganeh DF, Sander LE, Erschfeld S, Giebeler A, Liedtke C, Wasmuth HE, Trautwein C, Streetz KL** 2010 Lack of interleukin-6/glycoprotein 130/signal transducers and activators of transcription-3 signaling in hepatocytes predisposes to liver steatosis and injury in mice. Hepatology 51:463–473
55. **Horiguchi N, Wang L, Mukhopadhyay P, Park O, Jeong WI, Lafdil F, Osei-Hyiaman D, Moh A, Fu XY, Pacher P, Kunos G, Gao B** 2008 Cell type-dependent pro- and anti-inflammatory role of signal transducer and activator of transcription 3 in alcoholic liver injury. Gastroenterology 134:1148–1158
56. **Puri P, Mirshahi F, Cheung O, Natarajan R, Maher JW, Kellum JM, Sanyal AJ** 2008 Activation and dysregulation of the unfolded protein response in nonalcoholic fatty liver disease. Gastroenterology 134:568–576
57. **Ozcan U, Yilmaz E, Ozcan L, Furuhashi M, Vaillancourt E, Smith RO, Görgün CZ, Hotamisligil GS** 2006 Chemical chaperones reduce ER stress and restore glucose homeostasis in a mouse model of type 2 diabetes. Science 313:1137–1140
58. **Lawler Jr JF, Yin M, Diehl AM, Roberts E, Chatterjee S** 1998 Tumor necrosis factor-α stimulates the maturation of sterol regulatory element binding protein-1 in human hepatocytes through the action of neutral sphingomyelinase. J Biol Chem 273:5053–5059
59. **Ma KL, Ruan XZ, Powis SH, Chen Y, Moorhead JF, Varghese Z** 2008 Inflammatory stress exacerbates lipid accumulation in hepatic cells and fatty livers of apolipoprotein E knockout mice. Hepatology 48:770–781